AN EXPERIMENTAL INVESTIGATION OF VISCOUS EFFECTS ON STATIC AND IMPACT PRESSURE PROBES IN HYPERSONIC FLOW

Thesis by

Malcolm L. Matthews

In Partial Fulfillment of the Requirements

For the Degree of

Aeronautical Engineer

California Institute of Technology

Pasadena, California

1958

ACKNOWLEDGMENTS

The author wishes to express his appreciation to his advisor, Dr. James M. Kendall, Jr., for his guidance and assistance throughout the work. He would also like to thank Professor Lester Lees for suggesting the project and for his interest in its progress and help at its conclusion.

The author is also greatly indebted to the Aeronautics machine shop for construction of the models and supporting equipment; to the staff of the hypersonic research group for their valuable assistance in performing the investigations; to Mrs. Mary Dennison for preparation of many of the figures; and to Mrs. Geraldine Van Gieson for comments on and typing of the manuscript.

ABSTRACT

An experimental investigation of viscous effects on static and impact pressure probes was conducted in the GALCIT Leg 1 hypersonic wind tunnel.

This investigation of the impact probes showed viscous effects to be important for free stream Reynolds numbers less than 6000 based on the probe diameter, in the Mach number range 5.4 to 5.7. For $80 < Re < 6000$, the results showed the measured impact pressure to be less than the inviscid value. The maximum deviation from the inviscid impact pressure was 2.3 per cent at a Reynolds number of 200. For $Re < 80$ the measured impact pressure was greater than the inviscid value.

The investigation of the static pressure probes for a Mach number 5.8 and a free stream Reynolds number of 16,000 based on the probe diameter showed a very thick and rapidly growing boundary layer over the probe surface. This boundary layer was sufficient to cause the static pressure measured by a 10 degree cone-nosed probe with its orifice 45 diameters aft of the probe tip to be 7.5 per cent greater than the free stream static pressure. The boundary layer thickness on the 10 degree cone-nosed probe was several times that of the probe radius. The boundary layer was surveyed on a hemispherical-nosed and a flat-nosed probe and showed the boundary layer thickness to be several times that of the 10 degree cone-nosed probe.

TABLE OF CONTENTS

LIST OF FIGURES

LIST OF SYMBOLS

a	velocity of sound, $\sqrt{\gamma RT}$, ft./sec.
d	probe outside diameter, inches
L	characteristic length, inches
M	Mach number, u/a, dimensionless
p	pressure, lbs./sq. in
p_s	static pressure, lbs./sq. in.
r	radius measured from probe centerline, inches
r_o	radius of probe, d/2, inches
R	gas constant for air, 1716 ft.^{2}/(sec.^{2})(deg. F)
Re	Reynolds number, $\rho uL/\mu$, dimensionless
T	absolute temperature, degree R
u, v, w	local velocity parallel to x, y, and z coordinates, respectively, ft./sec.
U	free stream velocity, ft./sec.
x	distance aft of probe tip, inches, also streamwise coordinate
x_s	distance aft of cone shoulder on static probe, inches
y, z	transverse coordinates normal to x-axis
β	quantity defined by $\partial v/\partial y$, ft./(sec.)(ft.)
γ	ratio of specific heats, c_p/c_v, dimensionless
δ	boundary layer thickness defined by Figure 19. Also general boundary layer edge, inches
δ^*	boundary layer displacement thickness, inches
θ	inclination of streamlines, $d\delta^*/dx$, radians
μ	absolute viscosity, lb. sec./sq. ft.
ρ	mass density, lb. sec.^{2}/ft.^{4}

Subscripts

$( )_e$	refers to condition at edge of boundary layer
$( )_o$	refers to stagnation or reservoir conditions
$( )_\infty$	refers to undisturbed free stream conditions

Superscripts

$( )'$	condition after normal shock
$( )''$	conditions measured by impact-pressure probe

I. INTRODUCTION

Local flow properties in supersonic wind tunnels are usually determined by means of static and impact pressure probes. In regions of isentropic flow where the reservoir pressure (p_o) and total temperature (T_o) are known, the flow properties can be completely determined by measuring the impact pressure. In regions of non-isentropic flow the impact pressure is not enough to describe the flow because the true total pressure (the pressure recovered by an isentropic compression to zero velocity) is not known, and it is necessary to have another independent measurement such as mass flow or static pressure. An example of a region of constant total pressure is the undisturbed flow in a wind tunnel, whereas if curved shocks are present or wakes behind blunt bodies, or boundary layer, etc., the impact pressure is not constant. However, the investigation of boundary layer flow is usually accomplished by measuring the local impact pressure through the boundary layer and the static pressure on the surface of the body, and then assuming the static pressure to be constant across the boundary layer.

When the details of the flow field are of interest it is often necessary to employ very small impact and static pressure probes and the question of viscous effects naturally arises, especially in regions of low velocity.

At hypersonic Mach numbers the flow in the stagnation-point

region of an impact pressure probe can certainly be regarded as incompressible for a first approximation. In that case the analysis of viscous effects for incompressible flow given in Reference 1 is applicable except that flow quantities must be evaluated behind the normal shock. Consider an impact probe oriented along the x-axis with its vertex at the origin, The radial coordinate is y measured from the x-axis, and the oncoming flow is parallel to the x-axis. The flow behind the normal shock along the central streamline leading to the stagnation point decelerates to zero velocity at the nose of the probe. The Navier-Stokes equation along the stagnation streamline ($y = v = \frac{\partial^2 u}{\partial y^2} = 0$) reduces to the following form

$$\rho u \frac{\partial u}{\partial x} = - \frac{\partial p}{\partial x} + \mu \frac{\partial^2 u}{\partial x^2}$$

If the probe nose is at stagnation temperature the density and viscosity are very nearly constant across the boundary layer and this equation can be integrated with respect to x from $x = 0$ to the edge of the boundary layer δ. The result is

$$\frac{1}{2} \rho u^2 \Big|_0^\delta = - p \Big|_0^\delta + \mu \frac{\partial u}{\partial x} \Big|_0^\delta$$

Assuming that the flow does not slip over the surface, u, v, $\frac{\partial u}{\partial y}$, and $\frac{\partial u}{\partial x}$ all vanish at $x = 0$. Writing the measured impact pressure at the stagnation point as $p = p_o''$, we obtain

$$p_\delta + \tfrac{1}{2}\rho_\delta u_\delta^2 = p_o'' + \mu\left(\frac{\partial u}{\partial x}\right)_\delta .$$

The quantity $(p_\delta + \frac{1}{2}\rho_\delta u_\delta^2)$ is the inviscid impact pressure (p_o') outside the boundary layer. By the continuity equation,

$$\frac{\partial u}{\partial x} = -2\frac{\partial v}{\partial y} \equiv -2\beta$$

so that

$$p_o'' = p_o' + 2\mu\beta \quad \text{or} \quad p_o''/p_o' = 1 + \frac{2\mu\beta}{p_o'}$$

where β is the velocity gradient of the flow along the surface away from the stagnation point and is always greater than zero, therefore, $p_o''/p_o' \geq 1$ according to this analysis.

The quantity β may be determined theoretically or experimentally for a particular probe shape. At hypersonic speeds

$$p_o' \cong \rho_\infty U^2 , \quad \text{and} \quad \beta_{\text{inviscid}} \cong b\frac{U}{d}\sqrt{\frac{\rho_\infty}{\rho_o'}}$$

where $b = 2\sqrt{2}$ for a hemispherical nose, $b = \frac{8\sqrt{2}}{3\pi}$ for a flat nosed body[2]. By employing these approximations, one obtains

$$\frac{p_o''}{p_o'} \cong 1 + \frac{2b\sqrt{\frac{\rho_\infty}{\rho_o'}}}{Re'}$$

where $Re' = \frac{\rho_o' u' d}{\mu_o'} = \frac{\rho_\infty U d}{\mu_o'}$ is the Reynolds number based on quantities behind the normal shock. Of course some correction to β is required for the boundary layer thickness[1] and in fact $\beta = \beta_{\text{inviscid}}\left[1 + \frac{c}{\sqrt{Re'}}\right]$. Therefore, a somewhat more accurate expression for p_o''/p_o' is as follows:

$$\frac{p_o''}{p_o'} \cong 1 + \frac{2b\sqrt{\frac{\rho_\infty}{\rho_o'}}}{Re'} \left[1 + \frac{c}{\sqrt{Re'}}\right] .$$

In the absence of other effects, this expression should be valid down to values of Re' at which the boundary layer merges with the shock layer[3].

Impact pressure interpretation in subsonic and supersonic flow at low densities has been the subject of several other theoretical and experimental investigations[4-14]. Ipsen[4] analyzed the incompressible flow case of a prolate spheroid using potential flow, Stokes flow, and Oseen flow to approximate the viscous term of the Navier-Stokes equation for the stagnation streamline. He showed the viscous effects to be dependent on the inverse of the Reynolds number. Experimental investigations of impact probes in supersonic flow have been conducted by Kane and Maslach[5], Sherman[6], Enkenhus[7] for free molecule flow, and by Graves and Quiel[8] in hypersonic flow. Sherman[6] has shown that for Mach numbers 1.7 to 3.4 the viscous effects for internally chamfered probes are important for Reynolds numbers less than 200, based on the probe diameter and undisturbed free stream conditions. For free stream Reynolds numbers between 27 and 200, the measured impact pressure was less than the inviscid value, but it is greater than the inviscid pressure for Reynolds numbers less than 27. Graves and Quiel[8] have shown that for the same type probe in the Mach number range 5.3 to 5.6, the viscous effects are important for Reynolds numbers less than 6000. The need for correction at such a high Reynolds number in the hypersonic case was difficult to understand; therefore, the present investigation was initiated to verify the results of Graves and Quiel

and to extend them to lower Reynolds numbers.

Static pressure probe readings may also be influenced by viscous effects at low Reynolds numbers. In hypersonic flow[15], the deceleration of the gas as it penetrates the viscous layer over a solid surface generates high temperatures in this region. As a result, the hypersonic laminar boundary layer is from 10 to 100 times thicker than at low speeds at the same Reynolds number, and the outward deflection induced by the thick boundary layer is equivalent to a modification of the body shape. At high speeds, even small changes in the flow direction result in large pressure changes. Such a body, being used as a static pressure measuring device, would need correction as a result of the pressure induced by the boundary layer growth.

Several experimental investigations have been conducted to determine the viscous effects on static pressure probes. Talbot[16] investigated the viscous effects on a series of geometrically similar cones in rarefied gas flow over a Mach number range $3.69 < M < 4.13$ and a Reynolds number range $917 < Re/inch < 3590$. His data indicated that viscous effects increase linearly with increasing orifice diameter and also increase almost as $1/\sqrt{Re_x}$. Schaaf, Hurlbut, and Talbot[17] conducted experiments on a series of blunt-nosed cones in rarefied gas at a Mach number 5.8 to determine the pressure distributions. An indication of the viscous effects could be obtained by comparing their results with those of Machell and O'Bryant[18] for geometrically similar models at the same Mach number but much higher Reynolds numbers. Comparison showed essentially no viscous effects on the surface pressure.

The present investigation of static pressure probes was exploratory in nature. An attempt was made to clarify the main aspects of the problem. The main emphasis was placed on the investigation of the impact probes.

II. EQUIPMENT AND PROCEDURE

A. Wind Tunnel Description

The static and impact pressure probe experiments were conducted in the Leg 1 wind tunnel of the GALCIT hypersonic facility. This tunnel is of the continuous flow, closed return type, with a nominal Mach number of 5.8 and a test section size of 5 x 5 inches. The reservoir pressure (p_o) ranges between 10 psia and 89 psia corresponding to Reynolds numbers (Re) between 24,000 and 194,000 per inch. The reservoir pressure is controlled to within accuracy limits of $\pm$ 0.2 psi. The reservoir temperature is limited to about 300^{o}F and is controlled to within $\pm$ 2^{o}F. A complete description of the compressor plant and the associated instrumentation may be found in References 19 and 20.

The flow in the test section is axially uniform starting at a point 22 inches aft of the throat and extends four inches downstream. The flow inclination in this region is less than $\pm$ 0.1 degrees.

B. Model Descriptions

1. Impact Pressure Probes

Eight probes were used in this phase of the investigation. Their outside diameters ranged from 0.0028 inches to 0.25 inches. The probes were flat-ended with a ratio of orifice diameter to outside diameter of approximately 0.4. The probe geometry was determined such that construction of the smallest probes would be practical. It would have been extremely difficult (if not impossible) to make the smallest probes with various nose geometries.

The probes with diameters 0.016, 0.032, 0.064, 0.125, and 0.25 inches were made of stainless steel and were mounted in two wedge-shaped rakes. (See Figure 1.) The rakes were mounted in the tunnel on the externally-operated model control system. (See Figure 2.)

The probes with diameters 0.0028, 0.0043, and 0.0088 inches were made of pyrex tubing drawn to a suitable dimension. The flat end of each probe was made by breaking the tube and examining it with the aid of a Kodak Contour Projector with magnification factor of 100. Since the nose condition determines the shape of the shock wave and the pressure behind it, the probes were not considered satisfactory unless the nose was square and flat, as shown in Figure 3. A cross-section of one pyrex probe is shown in Figure 4.

To keep the response time of the manometer low, it was necessary to minimize the length of the small diameter probes; therefore, the probe tips were made approximately 0.2 inches in length. The volume within the manometer and connecting tubing was held to a minimum by devising a manometer small enough to be mounted in the test section. (See Figure 5.) By means of this manometer, it was possible to measure the difference between the probe impact pressure and a reference impact pressure.

The probe-holder-manometer incorporated two pyrex manometer tubes, one connected to an 0.125 inch reference probe and the other to the pyrex probe mounted diametrically opposite. (See Figure 9.) The entire manometer could be rotated to bring either probe in line with the airstream. The base of the manometer was an "O" ring valve designed to transfer the fluid to the manometer tube connected

to the probe in the forward position. Each of the manometer tubes formed one leg of a "U" tube when rotated to the forward position, the other leg being a supply line to a vacuum-referenced reservoir. The fluid in this manometer was silicone fluid with a viscosity rating of 10 centistokes. A cathetometer was used to measure the fluid height in the manometer.

2. Static Pressure Probes

Three groups of probes were tested with nose cones of total angle equal to 5, 10, and 20 degrees, respectively. (See Figure 6.) The probes were constructed of 0.083-inch outside diameter stainless steel tubing and the nose cones were made of solid stainless steel. To obtain the static pressure distribution aft of the cone tip, each cone probe was constructed with an orifice at a particular distance aft of the cone vertex. The 10 degree cone group consisted of four probes with orifices located 10, 15, 25, and 45 diameters, respectively, from the cone vertex. The four probes in the 20 degree cone group had orifices in similar locations to the 10 degree cone group. The 5 degree cone group consisted of three probes with orifices located 15, 25, and 45 diameters, respectively, from the cone vertex. A support to hold one probe was made of stainless steel and was attached to the model actuators in the test section, as shown in Figure 7.

C. Procedure

1. Impact Pressure Probes

The impact probe rakes were mounted on the model control

actuators so that the flat end of each probe was at a point 22 inches aft of the tunnel throat. The rake was then connected to a multi-tube silicone manometer[20] and the complete system checked for leaks. With the tunnel operating at specified reservoir conditions, each probe in the rake was moved to the tunnel centerline, and the impact pressure measured. The vertical position of all probes on the centerline was checked by observing them by means of a cathetometer. The pressure measured by each probe was checked for repeatability.

The probe-holder-manometer was mounted on the removable block in the tunnel floor; the silicone supply tube and knob for rotating the manometer extended below. The flat end of each small probe in the probe-holder was located at a point 21 inches aft of the tunnel throat because of the position of the removable floor block. With the block in place the system was checked for leaks. A pyrex probe was set in the probe-holder, sealed with glyptal and baked with an infrared heat lamp. With the tunnel operating at the specified reservoir conditions and the pyrex probe in the forward position, the silicone reservoir was raised to a height such that the meniscus of the silicone was at a suitable place in the manometer tube. Sufficient time was allowed for manometer equilibrium, and the reading of the silicone height was recorded. Equilibrium reading for the smallest probes could be achieved in a time as short as 5 to 10 minutes with proper adjustment of the reservoir height. While the silicone reservoir was held at a constant height, the manometer was rotated 180 degrees to bring the reference probe to the forward position. When equilibrium had been reached, the manometer reading was taken. The difference between

the two readings was the difference between the reference impact pressure and the impact pressure of the pyrex probe.

With the reference probe remaining in forward position, the silicone fluid supply tube was replaced by a tube leading to the silicone fluid manometer board and the absolute reference pressure read. The measured impact pressure was checked to determine the repeatability. The data was reduced to the ratio p_o''/p_o', where p_o'' is the measured impact pressure and p_o' is the impact pressure for the corresponding flow with no viscous effects. The inviscid impact pressure was obtained by the method of Sherman[6], which proved to be satisfactory. This technique consisted of plotting the measured impact pressure, for each flow condition, against the inverse of the probe diameter (1/d) for the stainless steel probes and extrapolating the curve to $1/d = 0$, which was considered to be the value for inviscid flow. This process is considered equivalent to letting the Reynolds number approach infinity, all other factors having been held constant.

The range of Reynolds number variation was achieved by varying the reservoir pressure from approximately 10.4 psia to 29.4 psia in addition to varying the probe diameter. By varying the pressure, the assumption that the Reynolds number is the main parameter for the investigation could be checked.

Since the manometer tubes were inside the test section and the silicone fluid subject to a temperature of approximately 200°F, the density of the silicone was corrected to room temperature. The maximum correction was about 0.1 per cent of the impact pressure.

2. Static Pressure Probes

The tips of the probes were located at a point 22 inches aft of the throat in the region of uniform flow. The static pressures (p_s) were measured on the silicone manometer board for each of the eleven static pressure probes. The free stream static pressure (p_∞) was calculated from the measured impact pressure using tables in Reference 21. The tunnel operating conditions for this phase of the investigation were a reservoir pressure of 88.4 psia and a reservoir temperature of 225°F. Interference effects from the support feeding forward through the boundary layer were investigated and found to be negligible for the present case.

3. Determination of Flow Parameters

The Mach number of the flow was determined from the ratio of the measured impact pressure corrected for viscous effects (p_o') to the tunnel reservoir pressure (p_o), by means of tables in Reference 21.

The Reynolds number was computed for each flow setting and is defined as,

$$Re = \frac{\rho u L}{\mu}$$

where ρ, u, and μ are evaluated for a particular flow condition; i. e., free stream or for flow behind a normal shock, and L is some characteristic dimension. Using the definition of Mach number, the equation of state for a perfect gas, the isentropic relation for the velocity of sound, and with units given in the list of symbols, the relation reduces to

$$Re = 0.343 \frac{M p L}{\mu \sqrt{T}}$$

Reynolds number based on free stream flow properties is designated by Re, and the characteristic dimension was taken to be the probe outside diameter. The viscosity of air at very low temperatures is given by Keyes' equation

$$\mu = 2.316 \times 10^{-8} \frac{T}{1 + \frac{219.8}{T} 10^{-(9/T)}} .$$

Reynolds number based on conditions behind a normal shock is designated by Re', and the characteristic dimension was taken to be the probe outside diameter. The conditions behind a normal shock were computed using the tables of Reference 21.

III. RESULTS AND DISCUSSION, IMPACT PRESSURE PROBES

The results for the impact pressure variation with free stream Reynolds number based on the probe diameter are shown in Figure 10. These results show that impact pressure probes are sensitive to effects of viscosity for Reynolds numbers less than 6000 in the present Mach number range. For free stream Reynolds numbers between 80 and 6000, the measured pressure is less than the inviscid pressure and for Reynolds numbers below 80, the measured pressure is greater than the inviscid value. In this investigation, the maximum deviation of the measured impact pressure from inviscid value was about 2.3 per cent at a Reynolds number of 200.

Previous experimental investigations have been conducted on probes of different geometry from those in the present test. Comparison of the present results with the 10 degree internally-chamfered probe data of Graves and Quiel[8] for a nominal Mach number 5.6, shows the two sets of measurements to be in excellent agreement. (See Figure 11.) Thus, comparison with other data for probes with geometry similar to those of Graves and Quiel but at different Mach numbers is justified. The comparison between the present results and those of Graves and Quiel verifies the existence of viscous effects at Reynolds numbers as high as 6000. The present data indicate qualitative agreement with the work done by Sherman[6] at Mach numbers from 1.7 to 3.4. The data indicate similar trends, but the viscous effects are important at a much higher Reynolds number and also the viscous effects are larger.

The impact pressure variation with Reynolds number (Re') based on flow conditions behind a normal shock is shown in Figure 12.

Figure 13 shows a comparison between the present results and the work of Sherman on the same basis.

To summarize: when the Reynolds number behind the normal shock is greater than 100 the viscous correction to the measured impact pressure is determined mainly by losses that are probably associated with the viscous flow around the sharp lip; when the Reynolds number behind the normal shock is less than 30 the viscous normal stress along the stagnation streamline begins to predominate and the lip losses become secondary as the Reynolds number decreases.

A limited investigation was conducted on three 0.016 inch diameter impact probes of different nose geometries, i.e., 10 degree internal chamfered, flat-ended, and hemispherical. The results obtained were essentially the same, within the scatter of the other data for the flow conditions tested, ($500 < Re < 900$). However, the effect of nose condition (rough and jagged) of the pyrex probes on the measured impact pressure was investigated and found to be critical and resulted in the strict requirements on the quality of the probes. (See Section II, page 8.)

IV. RESULTS AND DISCUSSION, EXPLORATORY INVESTIGATION OF STATIC PRESSURE PROBES

The three sets of static pressure probes, i.e., the three nose cone angles, were tested at a nominal Mach number 5.8. The probes were tested only at the highest reservoir pressure available, 74 psig. This condition corresponds to a Reynolds number of 194,000 per inch, or 16,000 based on the probe diameter and free stream conditions. The results of this survey are given in Figure 14 for the three nose cone angles. The free stream static pressure was calculated from the results of an impact probe with 0.083 inch diameter, which can be assumed to have no viscous effects.

Figure 14 shows that the static pressure measured by the static pressure probes differs considerably from the pressure given by inviscid flow theory. At a distance of 45 diameters from the cone vertex, the static pressure is on the average 7.5 per cent above the free stream value for the three nose cone angles.

Lees[15] concludes that the hypersonic boundary layer is many times thicker than that at lower speeds at the same Reynolds numbers, and the deflection of the streamlines induced by this thick boundary layer changes the effective shape of the body considerably. The small deflections of the streamlines produce large pressure changes at high speeds. The investigation of the boundary layer along a 10 degree cone-nosed static pressure probe was carried out by means of a flattened impact pressure probe with frontal height approximately 0.003 inches. The static pressure probe was mounted on a support from the

tunnel floor and the impact probe mounted on the model actuator supports. (See Figure 8.) Surveys were made at four stations located 10, 15, 25, and 45 diameters from the cone vertex to locate the boundary layer edge. The results of this investigation are given in Figure 15. The use of a blunt-nosed probe was suggested as a means of reducing the thickness of the boundary layer, the result being a better measure of the free stream static pressure. Therefore, boundary layer surveys were conducted for two other probes of different nose geometries, i. e., a flat-nosed probe and a hemisphere-cylinder probe, both made of 0.083 inch diameter stainless steel tubing. The results of these surveys are given in Figures 16 and 17. A comparison of the impact pressure profiles for the three probe types at x/d = 25 is shown in Figure 18.

An indication of the boundary layer thickness (δ) was obtained from the impact pressure profiles by using a definition given by Kendall[22] and is shown in Figure 19. The boundary layer growth for the three types of probes is given in Figure 20. The boundary layer displacement thickness (δ^*) for the 10 degree cone-nosed probe was calculated from the measured impact pressure surveys and the static pressure distribution along the probe (assuming isentropic flow behind the shock). The following equation given by Richmond[23] was used for this calculation:

$$(r_o + \delta^*)^2 - r_o^2 = \int_{r_o^2}^{(r_o + \delta^*)^2} \left(1 - \frac{\rho u}{\rho_e u_e}\right) d(r^2)$$

The boundary layer displacement thickness (δ^*) is compared with the

boundary layer thickness (δ) in Figure 20 (displacement thickness is dashed curve).

The survey showed the boundary layer on each of the probes tested to be very thick and its growth to be surprisingly linear with distance along the probe. The blunt-nosed probes were shown to have boundary layers several times that of the cone-nosed probe, contrary to the expected result. The rapid growth of the boundary layer results in a large induced pressure on the surface. By assuming the pressure across the boundary layer to be constant, an estimate of the induced pressure on the probes was easily made by means of the tangent cone approximation for the probe shape modified by the boundary layer displacement thickness, and the linearized equation for the pressure on a slender body, i.e.,

$$\frac{p_s - p_\infty}{p_\infty} = M^2 \theta^2 \left(\ln \frac{2}{M\theta} - \tfrac{1}{2} \right) ,$$

where $\theta = d\delta^*/dx$. For the 10 degree cone-nosed probe, at a distance of 45 diameters from the cone vertex, the induced pressure was calculated to be approximately 6 per cent above the free stream value, which is close to the experimentally observed value.

Kubota[24] has estimated the boundary layer growth on blunt nosed cylinders for very high Mach numbers to be $\delta^*/d \sim x/d$ as a first approximation. In the present case the Mach number is not considered very high, but the linearity of the measured boundary layer is an interesting comparison for the flat-nosed and hemispherically-nosed probes.

V. CONCLUSIONS AND RECOMMENDATIONS

The results of the static and impact pressure probe investigation indicate the following:

(1) Viscous effects on impact pressure probes are important for the flow conditions covered in this investigation for free stream Reynolds numbers below 6000 and $5.4 < M < 5.7$. The viscous effects result in a measured impact pressure less than the inviscid impact pressure for free stream Reynolds numbers between 80 and 6000. The maximum deviation was 2.3 per cent at a Reynolds number of 200. Below 80, the viscous effects result in a measured impact pressure greater than the inviscid value.

(2) The exploratory investigation of static pressure probes at Mach number 5.8 and free stream Reynolds number 16,000 based on the probe diameter shows that

(a) The boundary layer on the 10 degree cone-nosed probe at $x/d = 45$ gives a flow deflection, $d\delta^*/dx$, large enough to produce an induced pressure of approximately 7.5 per cent of the free stream static pressure.

(b) The boundary layer on the blunt-nosed probes was several times that of the 10 degree cone probes.

(c) The boundary layer grows approximately linearly with x for $10 < x/d < 45$ for all probes.

The recommendations for further investigations are the following:

(1) An investigation of various nose geometries should be

made for impact probes, such as flattened probes for use in boundary layer surveys in hypersonic flow.

(2) An extension should be made for the static pressure probe investigation in an effort to discover the correct parameters for representing the viscous effects. Probes of various geometries should be studied, e.g., blunt-nosed cones with the static orifices on the conical skirt, since the boundary layer effects would be reduced by the high pressure and negative pressure gradients.

REFERENCES

1. Chambre, P. L. and Schaaf, S. A.: "The Impact Tube". Vol. IX, High Speed Aerodynamics and Jet Propulsion Series, Princeton University Press, 1954.

2. Probstein, R. F.: "Inviscid Flow in the Stagnation Point Region of Very Blunt-Nosed Bodies at Hypersonic Flight Speeds". (Brown University), WADC TN 56-395 (ASTIA Document AD97273), ARDC, USAF, Wright-Patterson AFB, Ohio., Sept., 1956.

3. Lees, L.: "Recent Developments in Hypersonic Flow". Jet Propulsion, Vol. 27, No. 11, November, 1957, pp. 1162-1178.

4. Ipsen, D. C.: "Viscous Corrections to Impact Pressure on Prolate Spheroid". University of California, Report No. HE-150-89, March 12, 1952.

5. Kane, E. D. and Maslach, G. J.: "Impact-Pressure Interpretation in a Rarefied Gas at Supersonic Speeds". NACA TN 2210, 1950.

6. Sherman, F. S.: "New Experiments on Impact-Pressure Interpretation in Supersonic and Subsonic Rarefied Air Stream". NACA TN 2995, 1953.

7. Enkenhus, K. R.: "Pressure Probes at Very Low Densities". University of Toronto, Institute of Aerophysics Report No. 43, January, 1957.

8. Graves, J. C. and Quiel, N. R.: "Impact Pressure and Total Temperature Interpretation at Hypersonic Mach Number". GALCIT Hypersonic Research Project, Memorandum No. 20, July, 1954.

9. Kane, E. D. and Schaaf, S. A.: "Viscous Effects on Impact Probes in a Subsonic Rarefied Gas Flow". University of California, Report No. HE-150-82, March 9, 1951.

10. Chambre, P. L. and Smith, H. R.: "The Impact Tube in a Viscous Compressible Gas". University of California, Report No. HE-150-63, August 29, 1948.

11. Chambre, P. L.: "The Theory of the Impact Tube in a Viscous Compressible Gas". University of California, Report No. HE-150-50, November 1, 1948.

12. Chambre, P. A. and Schaaf, S. A.: "The Theory of the Impact Tube at Low Pressures". Journal of the Aeronautical Sciences, Vol. 15, No. 12, December, 1948, pp. 735-737.

13. Murphy, S.: "Evidence of an Inherent Error in Measurement of Total-Head Pressure at Supersonic Speed". Aeronautical Engineering Review, Vol. 12, No. 11, November, 1953, pp. 47-51.

14. Staros, B.: "Investigation of Effect of Energy Dissipation Behind a Detached Shock Wave on Total-Head Measurements". California Institute of Technology, Aeronautical Engineer Thesis, 1950.

15. Lees, L.: "Hypersonic Flow". Institute of the Aeronautical Sciences, Preprint No. 554, June, 1955.

16. Talbot, L.: "Viscosity Corrections to Cone Probes in Rarefied Supersonic Flow at a Nominal Mach Number of 4". University of California, Report No. HE-150-113, June 1, 1953.

17. Schaaf, S. A.; Hurlbut, F. C.; and Talbot, L.: "Pressure Distributions on Blunt-Nosed Cones in Hypersonic Low Density Flow". Bell Aircraft Report No. D143-978-101, April 30, 1957.

18. Machell, R. M. and O'Bryant, W. T.: "An Experimental Investigation of the Flow over Blunt-Nosed Cones at a Mach Number of 5.8". GALCIT Hypersonic Research Project, Memorandum No. 32, June, 1956. Also, Journal of the Aeronautical Sciences, Readers' Forum, Vol. 23, No. 11, November, 1956, pp. 1054-1055.

19. Eimer, M. and Nagamatsu, H. T.: "Direct Measurement of Laminar Skin Friction at Hypersonic Speeds". GALCIT Hypersonic Research Project Memorandum No. 16, July, 1953.

20. Baloga, P. E. and Nagamatsu, H. T.: "Instrumentation of GALCIT Hypersonic Wind Tunnels". GALCIT Hypersonic Research Project, Memorandum No. 29, July, 1955.

21. Ames Research Staff: "Equations, Tables, and Charts for Compressible Flow". NACA Report 1135, 1953.

22. Kendall, J. M., Jr.: "An Experimental Investigation of Leading Edge Shock Wave Boundary Layer Interaction". Journal of the Aeronautical Sciences, Vol. 24, No. 1, January, 1957, pp. 47-56.

23. Richmond, R. L.: "Experimental Investigation of Thick, Axially Symmetric Boundary Layers on Cylinders at Subsonic and Hypersonic Speeds". GALCIT Hypersonic Research Project, Memorandum No. 39, June, 1957.

24. Kubota, T.: "Investigation of Flow around Simple Bodies in Hypersonic Flow". GALCIT Hypersonic Research Project, Memorandum No. 40, June, 1957. Also, Heat Transfer and Fluid Mechanics Institute, June, 1957, pp. 193-210.

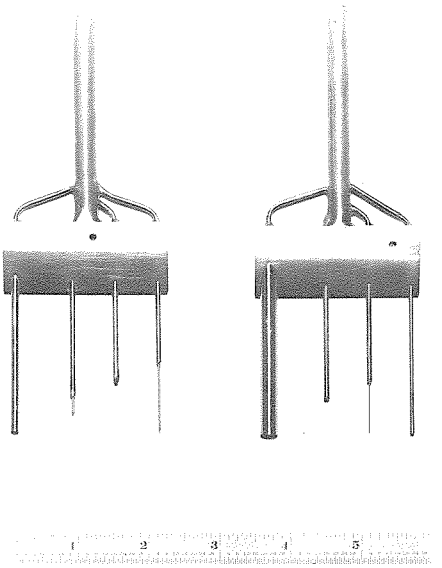

FIG. 1

IMPACT PRESSURE PROBE RAKES

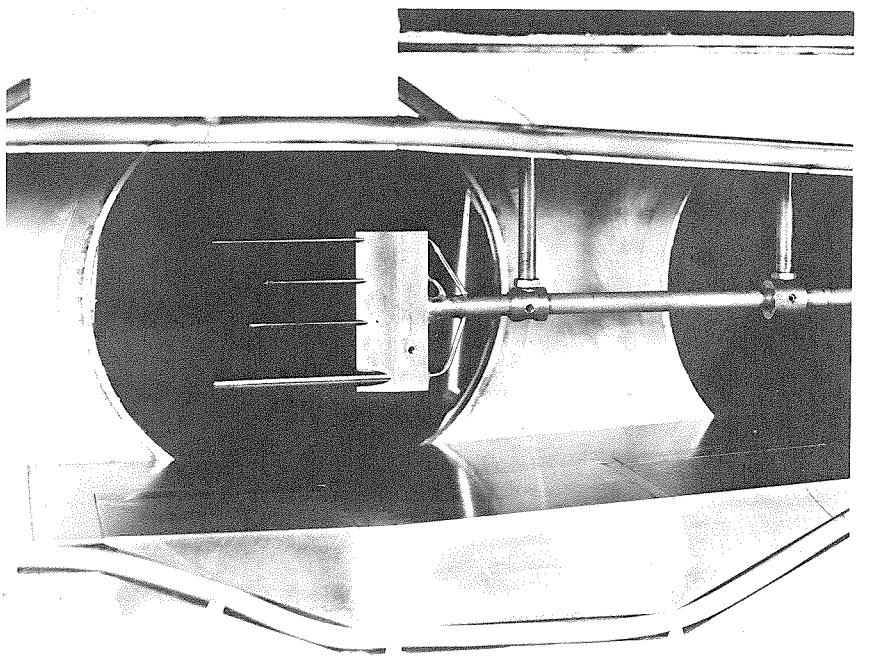

FIG. 2

IMPACT PRESSURE PROBE RAKE
IN HYPERSONIC WIND TUNNEL

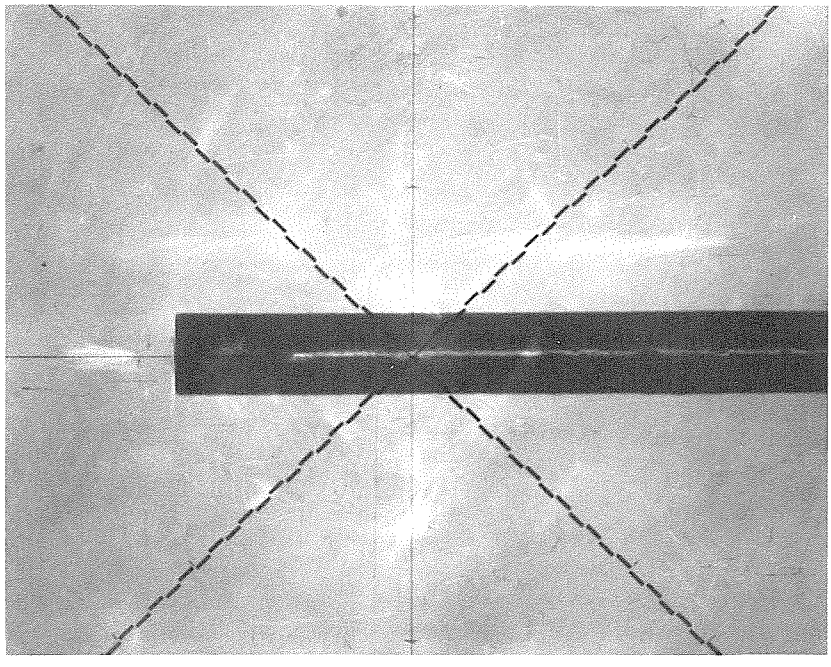

FIG. 3

SIDE VIEW OF 0.0088 INCH DIAMETER IMPACT PROBE
AS SEEN ON CONTOUR PROJECTOR

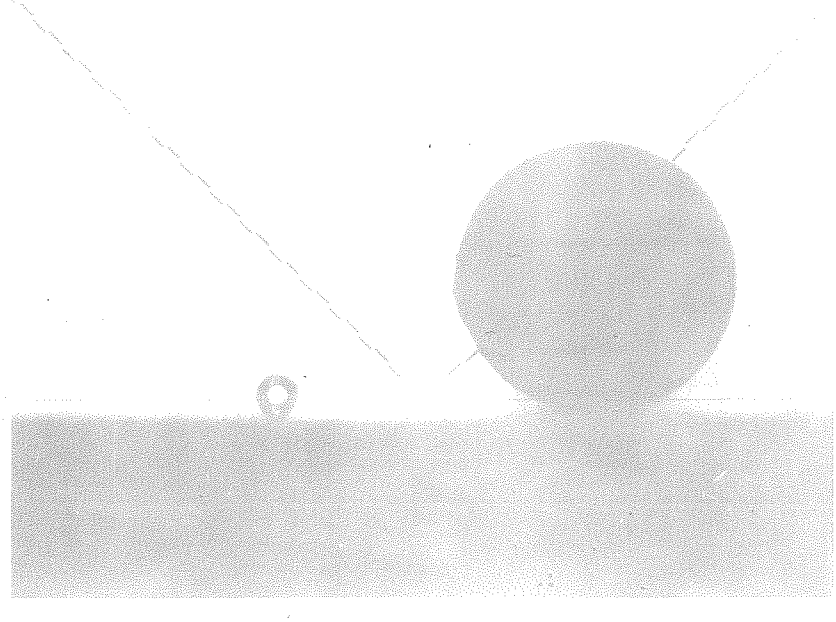

FIG. 4

END VIEW OF 0.0043 INCH DIAMETER IMPACT PROBE
COMPARED WITH STRAIGHT PIN

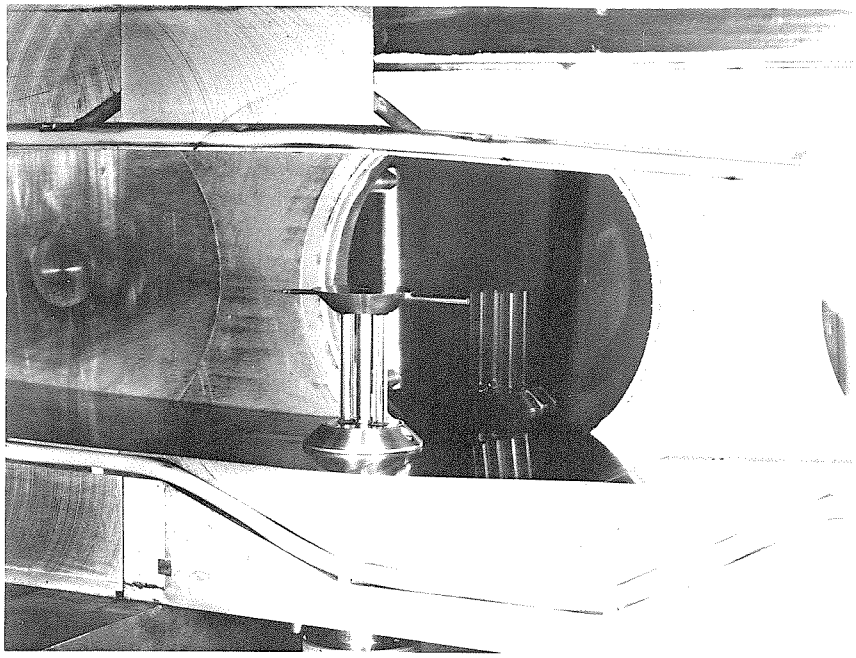

FIG. 5

PROBE-HOLDER-MANOMETER IN HYPERSONIC WIND TUNNEL

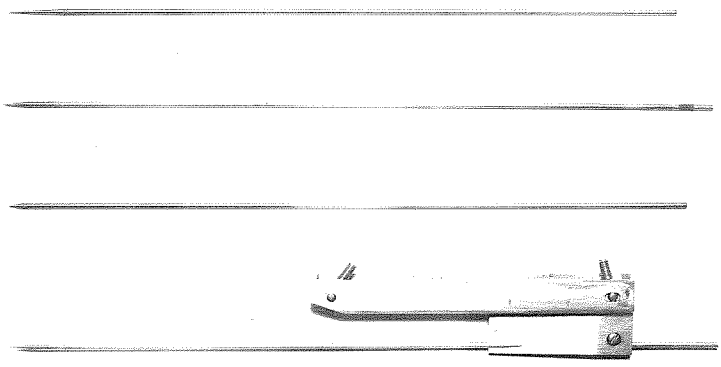

FIG. 6

STATIC PRESSURE PROBES AND SUPPORT

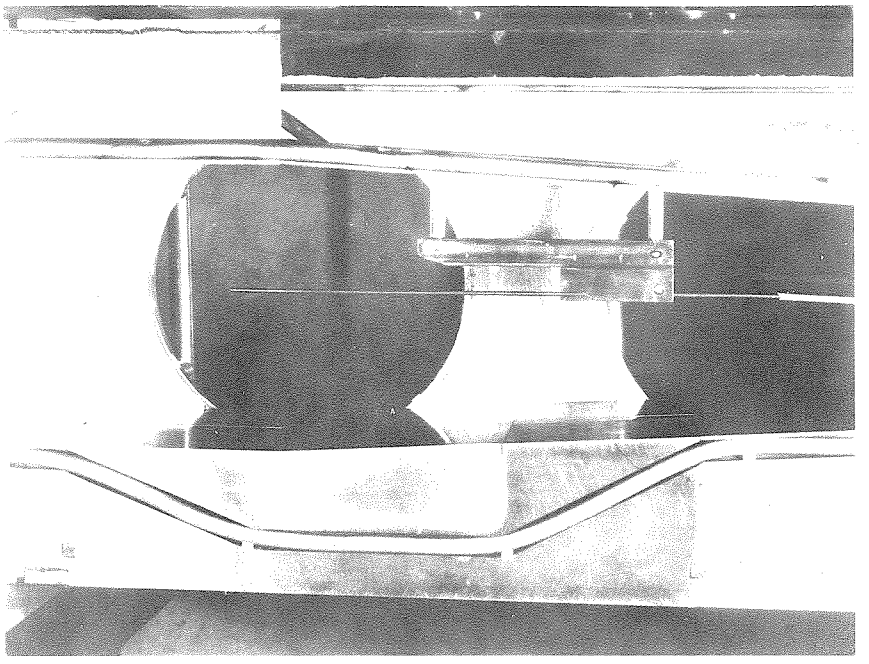

FIG. 7

STATIC PRESSURE PROBE AND SUPPORT
IN HYPERSONIC WIND TUNNEL

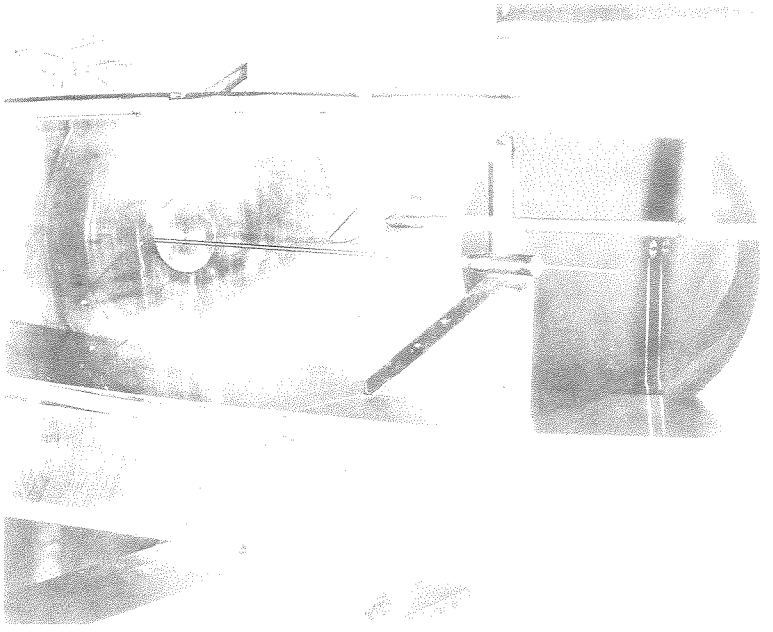

FIG. 8

BOUNDARY LAYER SURVEY EQUIPMENT
IN HYPERSONIC WIND TUNNEL

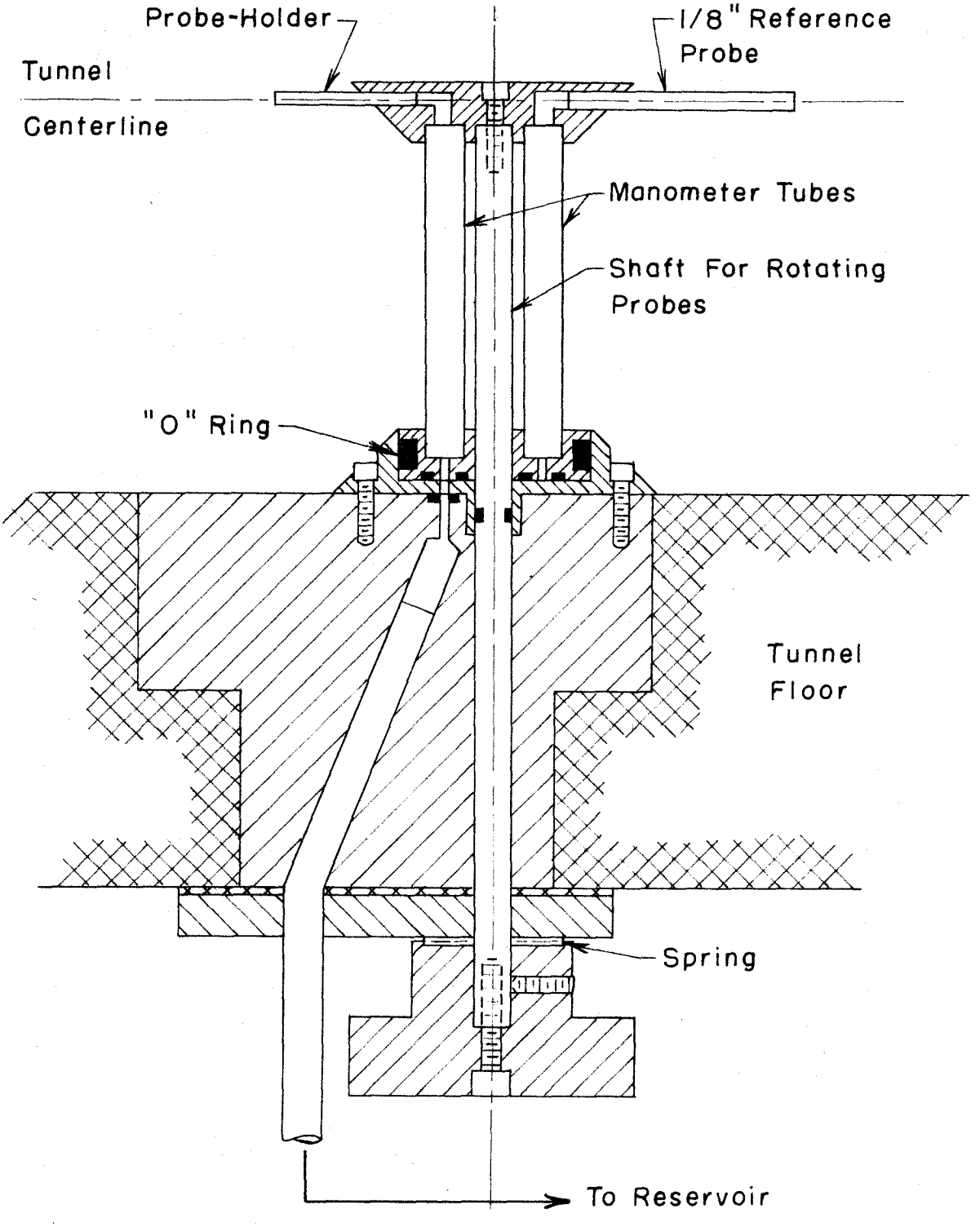

FIG. 9
SCHEMATIC OF THE PROBE - HOLDER - MANOMETER

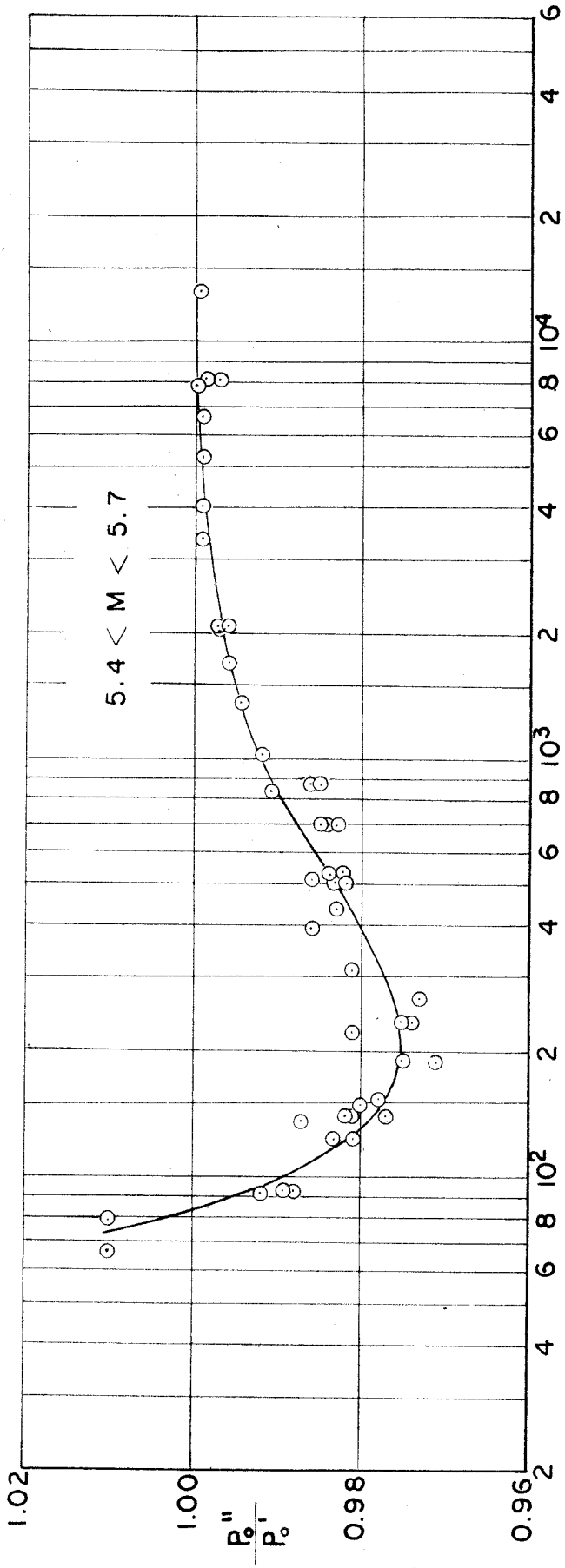

FIG. 10 VARIATION OF MEASURED IMPACT PRESSURE WITH FREE STREAM REYNOLDS NUMBER

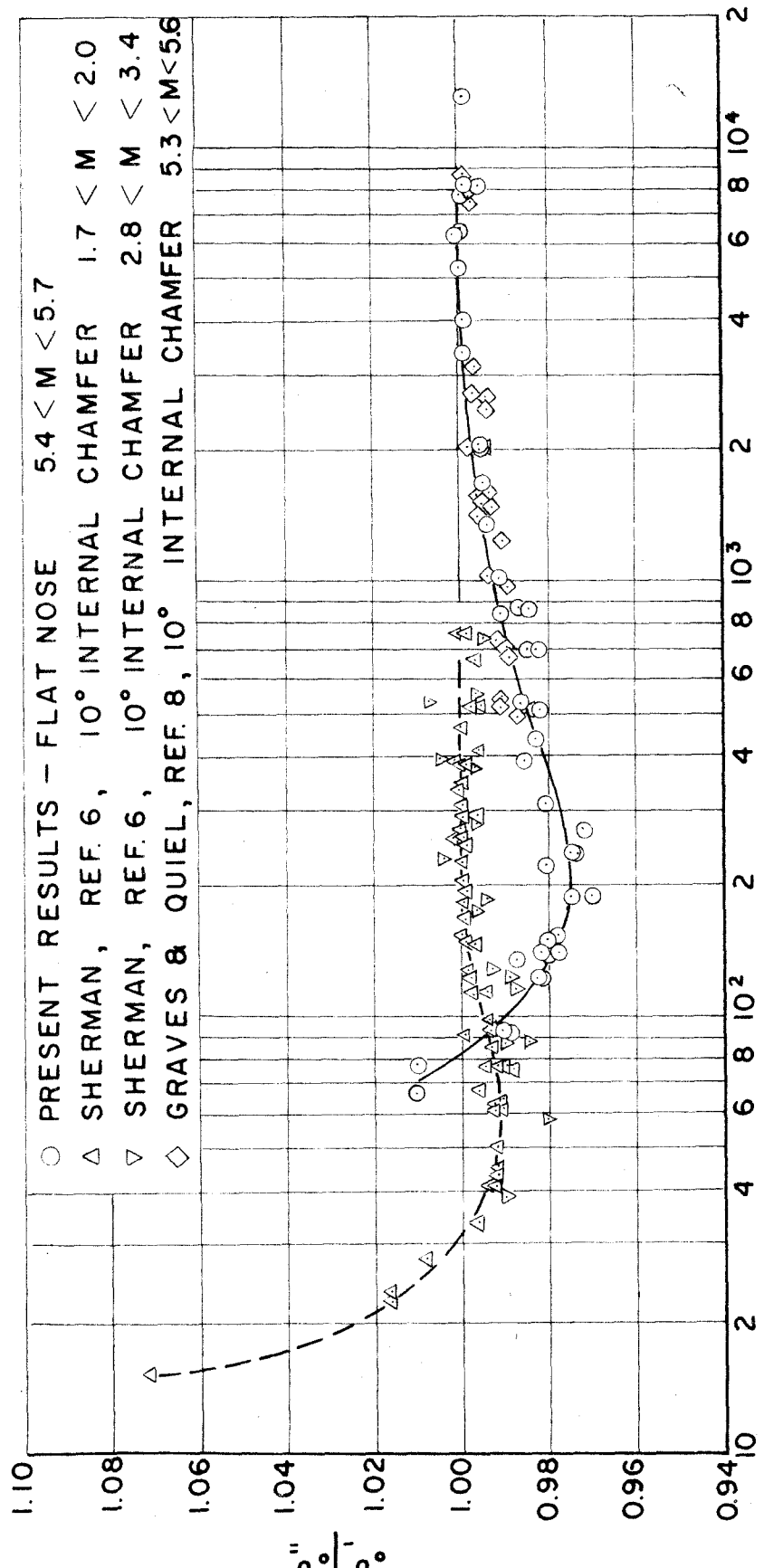

FIG. 11 COMPARISON OF THE VARIATION OF MEASURED IMPACT PRESSURE WITH FREE STREAM REYNOLDS NUMBER

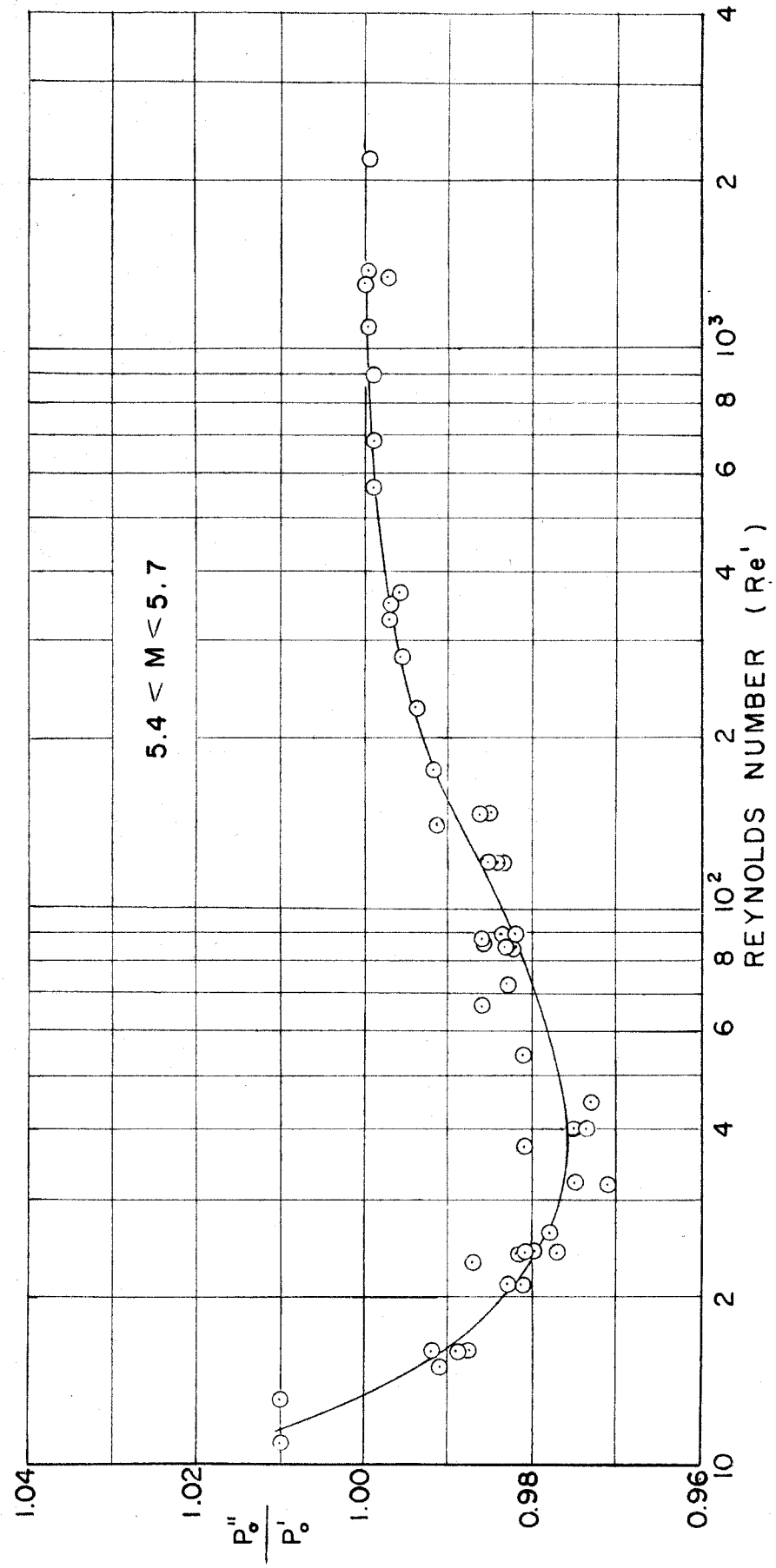

FIG. 12 VARIATION OF MEASURED IMPACT PRESSURE WITH REYNOLDS NUMBER BEHIND A NORMAL SHOCK

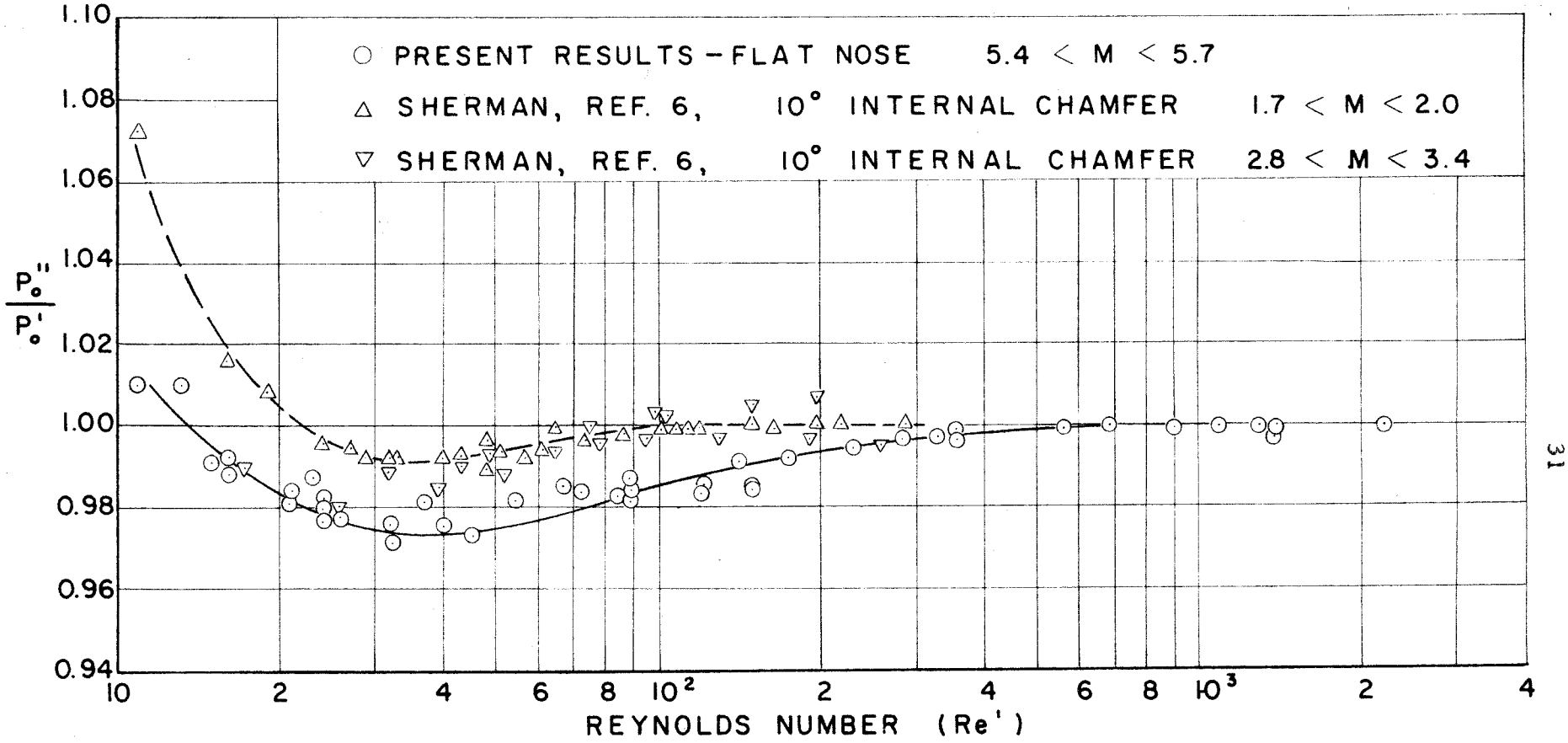

FIG. 13 COMPARISON OF THE VARIATION OF MEASURED IMPACT PRESSURE WITH REYNOLDS NUMBER BEHIND A NORMAL SHOCK

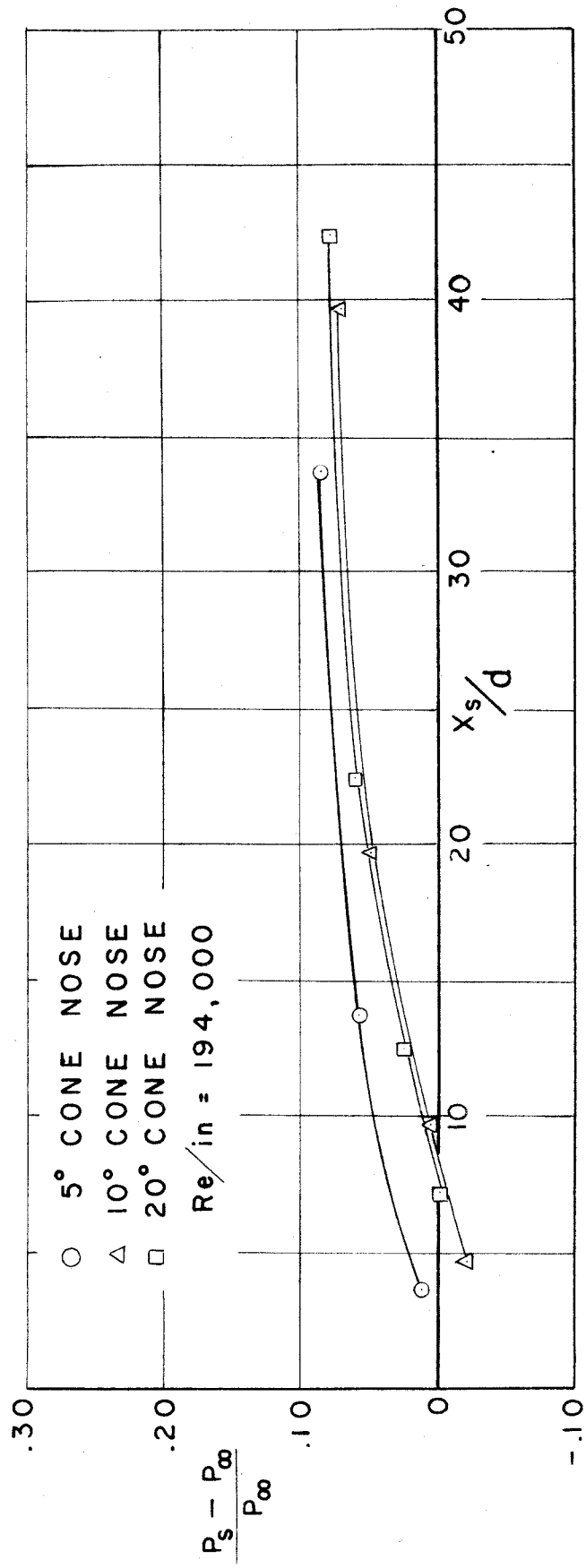

FIG. 14 PRESSURE DISTRIBUTION ON STATIC PRESSURE PROBES WITH VARIOUS NOSE CONE ANGLES

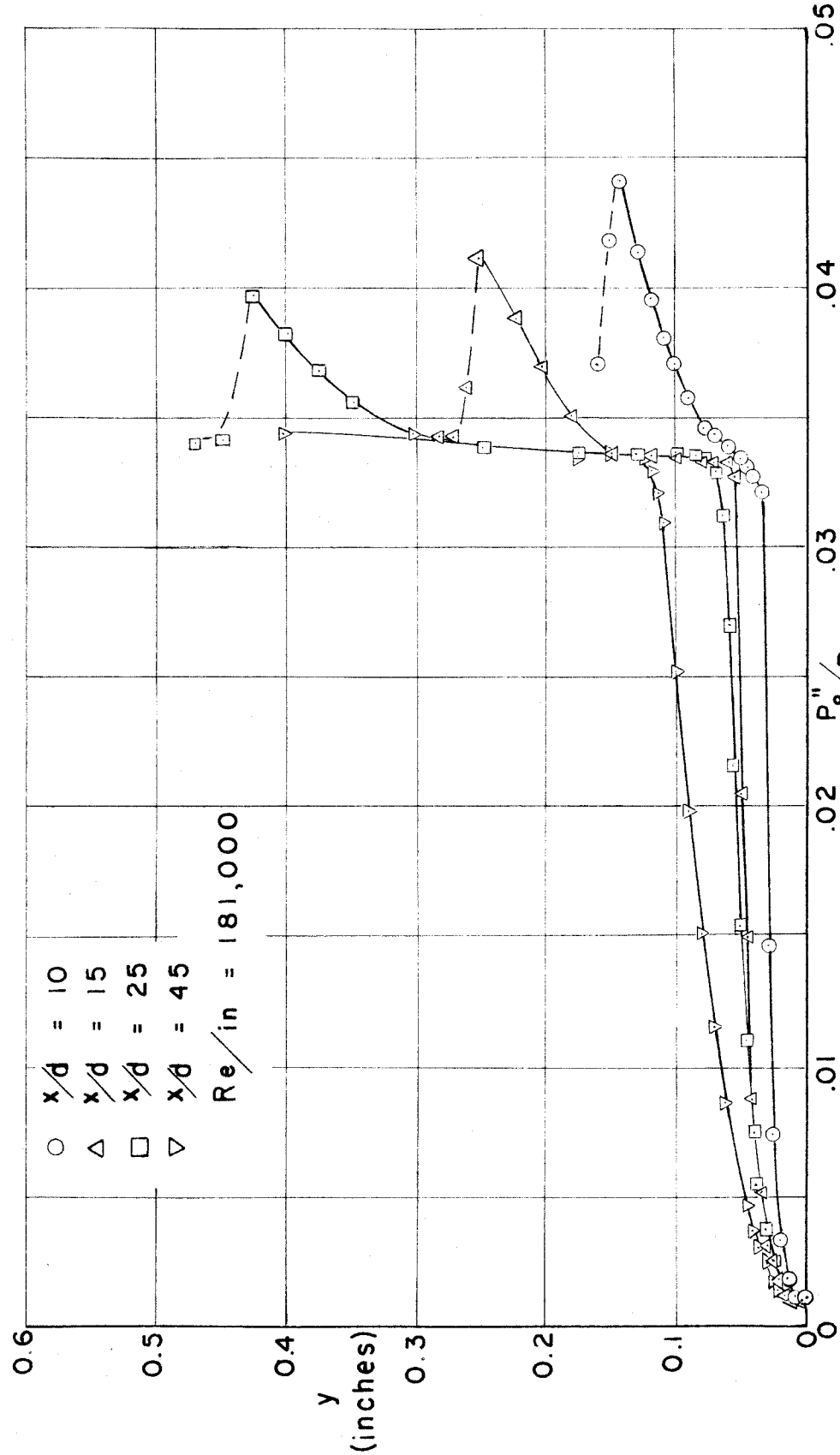

FIG. 15 IMPACT PRESSURE SURVEYS IN THE FLOW AROUND A 10° CONE-NOSE STATIC PRESSURE PROBE

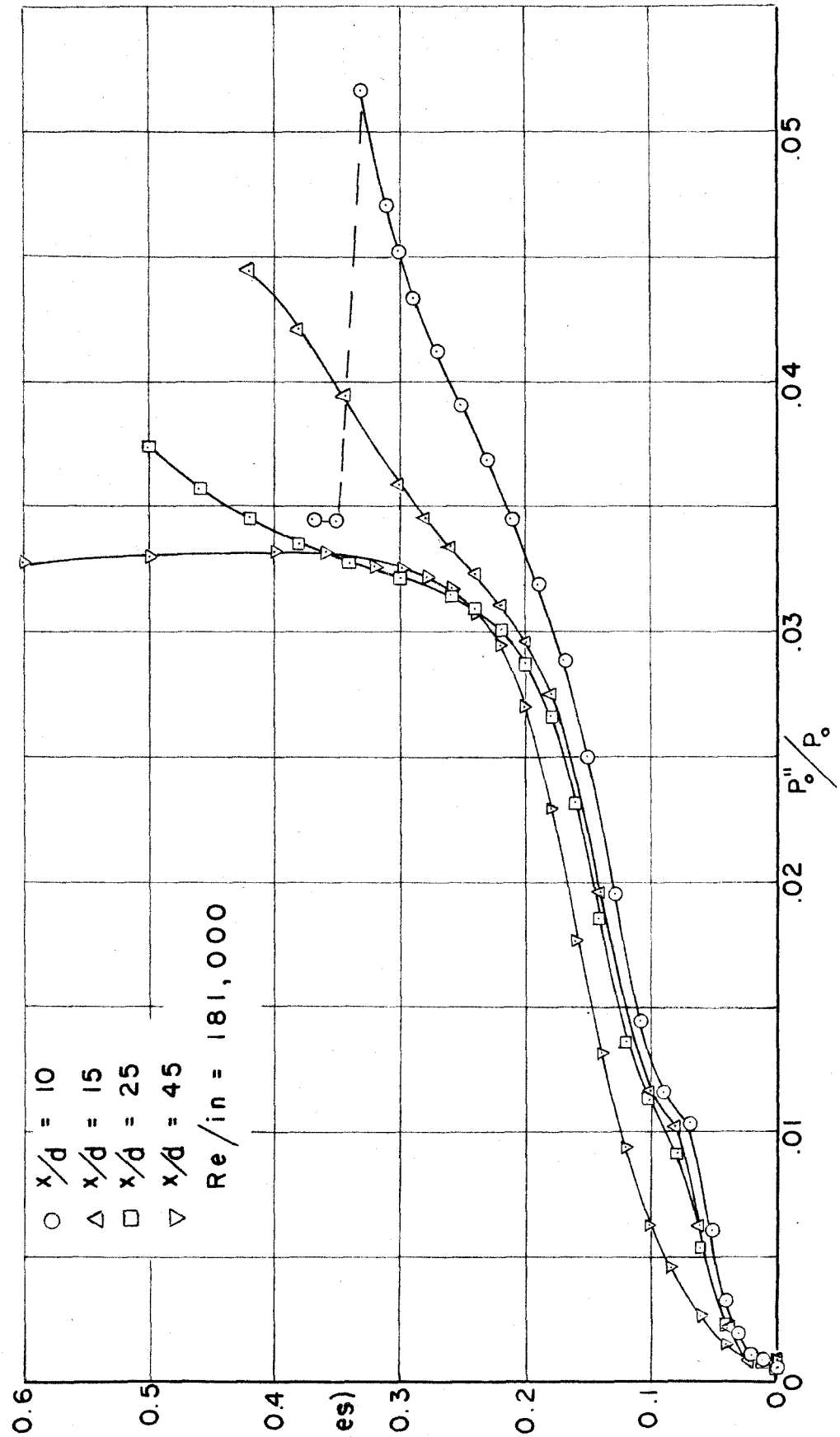

FIG. 16 IMPACT PRESSURE SURVEYS IN THE FLOW AROUND A FLAT-NOSE STATIC PRESSURE PROBE

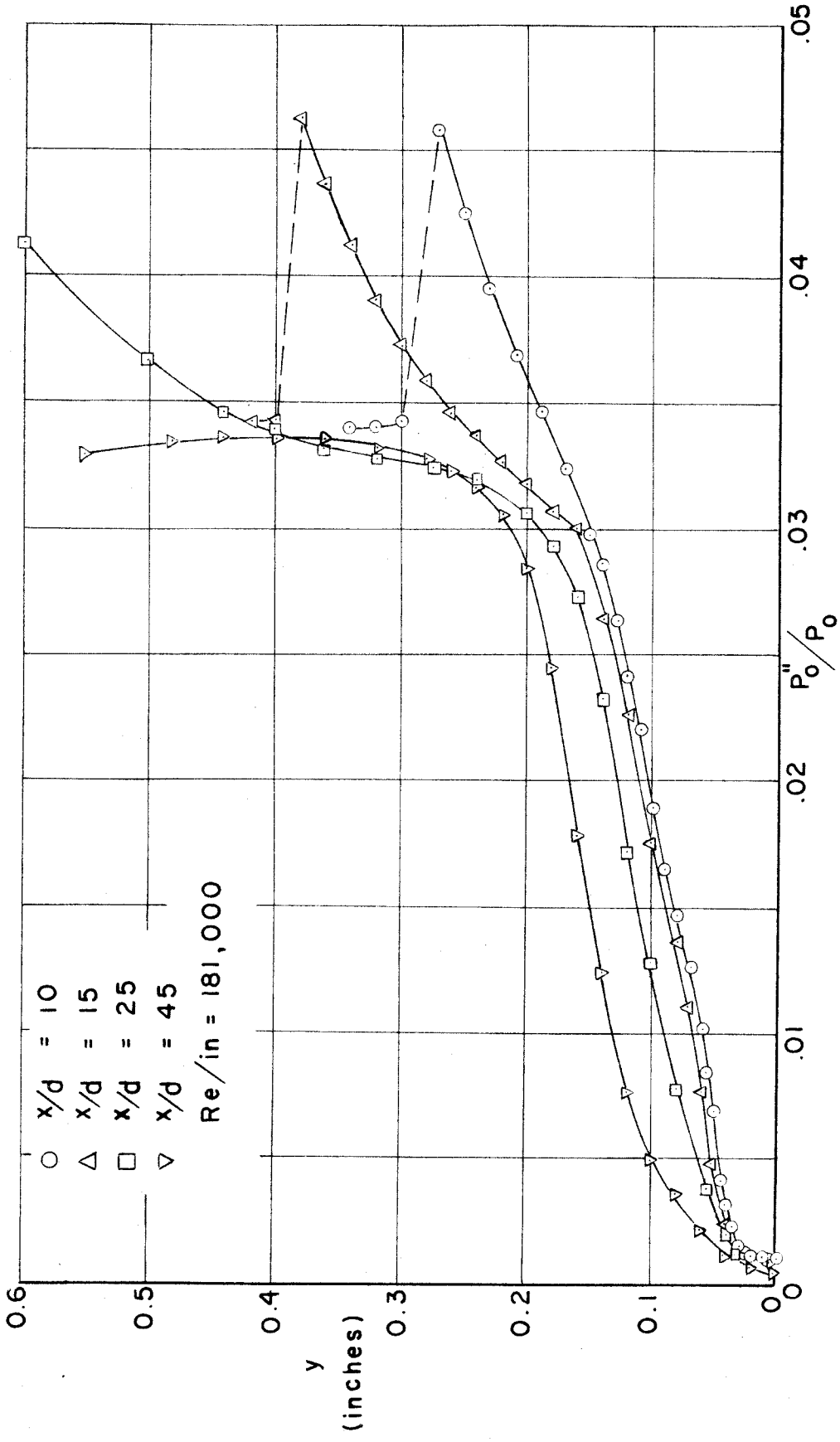

FIG. 17 IMPACT PRESSURE SURVEYS IN THE FLOW AROUND A HEMISPHERICAL-NOSE STATIC PRESSURE PROBE

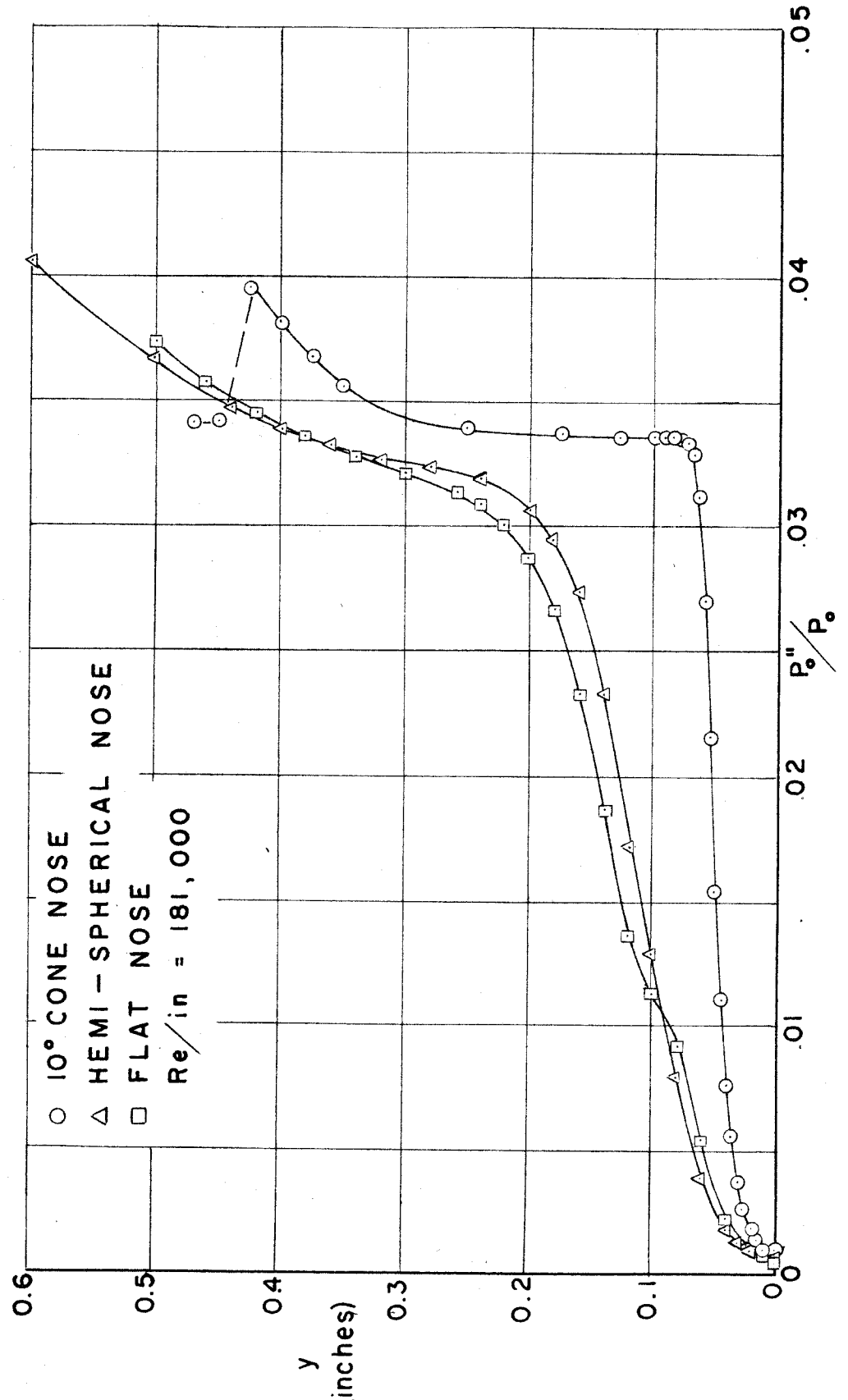

FIG. 18 IMPACT PRESSURE SURVEYS IN THE FLOW AROUND STATIC PRESSURE PROBES OF VARIOUS NOSE GEOMETRIES $x/d = 25$

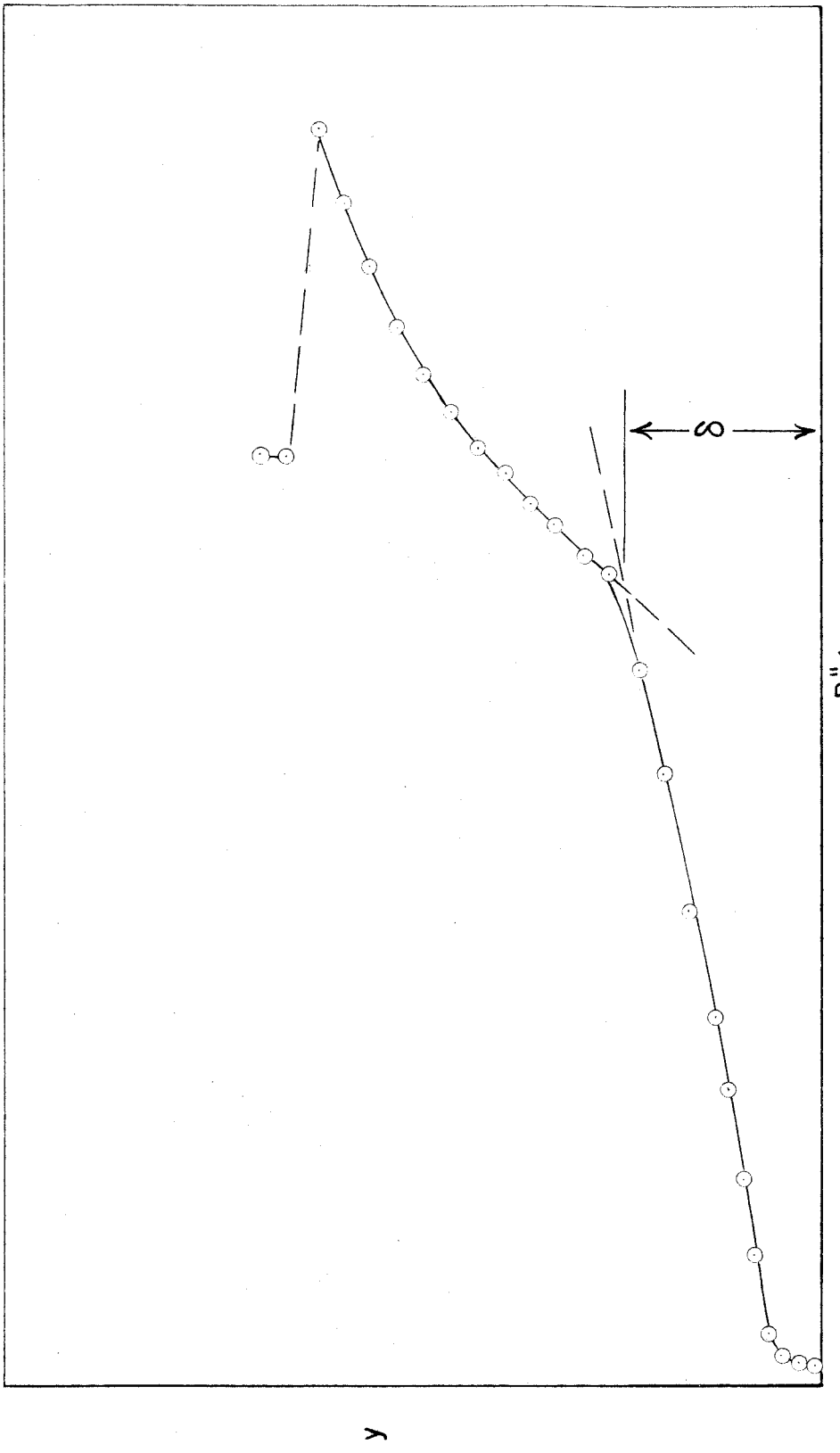

FIG. 19 DEFINITION OF BOUNDARY LAYER THICKNESS (δ)

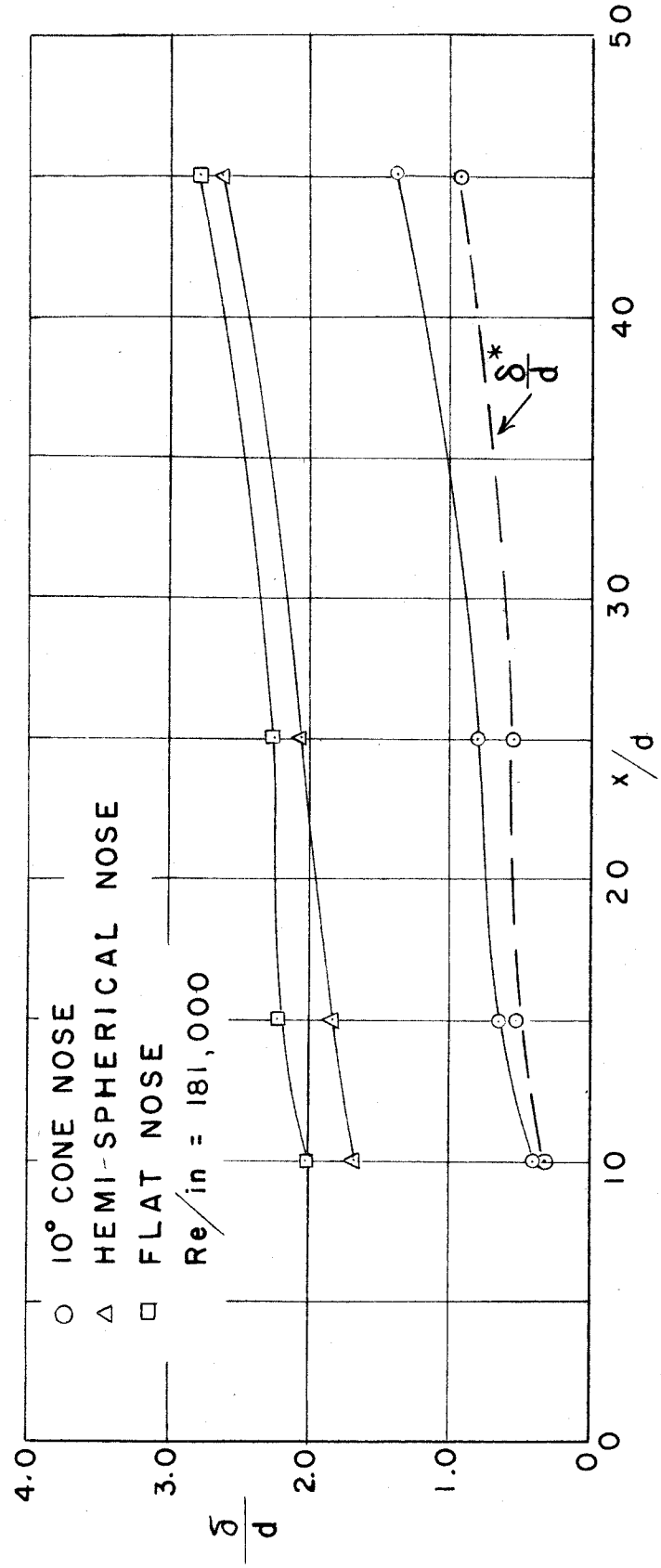

FIG. 20 BOUNDARY LAYER THICKNESS FOR STATIC PRESSURE PROBES OF VARIOUS NOSE GEOMETRIES